CSIRO

Indian Ocean yellowfin tuna close-kin mark-recapture design study

IOTC Working Party on Methods

Oct 2022

Rich Hillary, Laura Tremblay-Boyer, Ashley Williams, Nick Hill, Ann Preece

IOTC-2022-WPM13

Citation

Hillary RM, Tremblay-Boyer L, Williams AJ, Hill NJ, Preece AL (2022). Indian Ocean yellowfin tuna close-kin mark-recapture design study. Working Paper prepared for the 13th IOTC Working Party on Methods, 19-21 October 2021.

Contents

1   Abstract

Close-Kin Mark-Recapture (CKMR) is a genetics-based method for estimating key population metrics useful for independent assessment of stock status, or as data inputs for integrated stock assessment models, or as inputs to management procedures. This report evaluates a range of sampling scenarios for Indian Ocean yellowfin tuna to provide estimates of Total Reproductive Output (TRO, similar to spawning stock biomass), depletion in TRO, adult mortality and mean recruitment. This design study evaluates the sample sizes of juveniles and adults required to give precise estimates of these population metrics.

The analysis used a simplified population model that reproduced recent yellowfin tuna population dynamics, but in an equilibrium framework. Under these conditions, annual sampling levels of 25,000 to 30,000 samples were predicted to yield useful insights on population metrics with reasonable precision in the estimates. Specifically, the depletion in total reproductive output (TRO), could be estimated with a coefficient of variation (CV) of 15% with 30,000 annual samples over 5 years. After the initial 5 years are complete, a CKMR monitoring program would build on the existing data set to provide ongoing information for assessment and management.

2   Introduction

The Indian Ocean yellowfin tuna stock is estimated to be overfished and subject to overfishing (Fu et al. 2021). However, there is significant uncertainty in stock status due to long-standing issues, conflicts and inaccuracies in the data inputs and spatial structure used in the stock assessment (IOTC 2021). For instance, catches are not well documented for some fisheries, particularly artisanal fleets that harvest a large proportion of the yellowfin tuna catch. Therefore, it is difficult to obtain a reliable estimate of total fishing mortality. Also, standardised CPUE from longline fleets provide the main index of abundance, but it is unclear whether this index is reflective of abundance. This is due, at least in part, to operational changes in longline fishing (e.g., targeting, gear changes, new technology), fleet movements and declining longline effort which has led to significant gaps in spatial and temporal strata. The yellowfin tuna stock assessment will be externally reviewed in 2023 (see appendix 6c, IOTC 2021), but issues relating to uncertainty in the main data inputs will likely remain.

There is a need for improved approaches to estimate abundance that are independent of the current data inputs and biases associated with the current stock assessment. One promising alternative approach for an estimate of abundance that has been identified by the Indian Ocean Tuna Commission (IOTC) Scientific Committee is the application of close-kin mark-recapture (CKMR), a method with a proven track record in the assessment and management of Southern bluefin tuna (Bravington et al. 2016). CKMR data can also be integrated into assessments with other sources of data and can be used in management procedures (e.g., Hillary et al. 2019, 2020).

CKMR has been identified as a priority research activity for yellowfin tuna in the Working Party on Tropical Tuna (WPTT) Program of Work since 2017 (IOTC 2017). Kolody & Bravington (2019) concluded that CKMR should be logistically feasible for Indian Ocean yellowfin tuna provided that ample tissue samples can be obtained from appropriate locations and fisheries across the Indian

Ocean. They recommended that prior to an ocean basin-wide project, a detailed design study be undertaken that attempts to represent the biology more accurately and quantifies expected precision of different population parameter estimates with respect to sampling design. As such, this working paper outlines the preliminary results of a detailed CKMR design study for Indian Ocean yellowfin tuna.

3 Close-kin mark-recapture overview

CKMR uses modern genetics to identify closely related pairs of fish. The number of kin pairs identified and their distribution in space and time are used to estimate key population parameters such as absolute spawning biomass, total mortality, and connectivity (Bravington et al. 2016). CKMR is different to other types of mark-recapture approaches in that offspring 'tag' their parents via their DNA, and half-siblings 'tag' their shared parents via their shared DNA. CKMR requires collection of tissue samples for DNA extraction and genotyping, but these can be sampled from dead fish (i.e., fishery catches). In comparison to other mark-recapture approaches, there is no requirement to consider tag shedding, tag-induced mortality, mixing rates of tagged fish, or reporting rates of recaptured fish.

The concept of CKMR is based on the fact that every individual has exactly two parents (Bravington et al. 2016). For a given sample from a population, we would expect to find more parent-offspring pairs (POPs) in a smaller population than we would from a larger population. The probability that any random comparison between a juvenile and adult in the population is a parent-offspring pair can be expressed as:

$$\Pr(POP) = \frac{2}{N_{parents}}$$

where $N_{parents}$ is the total number of parents (mature individuals) in the population and the '2' represents the two parents of each offspring. The expected number of observed POPs, k, for a sample from the population can then be determined by summing the probabilities across all possible parent-offspring comparisons from the sample, such that:

$$k = \frac{2(m_{parents} \times m_{offspring}}{N_{parents}}$$

$$N_{parents} = \frac{2(m_{parents} \times m_{offspring}}{k}$$

where $m_{parents}$ and $m_{offspring}$ are the number of parents and offspring sampled from the population respectively.

The summary above is an oversimplification of the CKMR approach. Other factors that are considered in a real application include adult mortality in the interval between birth and sampling,

relative fecundity of fish by age or size, non-random sampling, and uncertainties with genotyping individuals (Bravington et al. 2016).

Another type of useful kin probability is the probability that any two individuals share a parent (i.e., they are half-siblings). Both types of kin probability depend on population dynamics for the stock, and so can be used to derive estimates of population parameters. Parent-offspring pairs and half-sibling pairs provide different information in CKMR population models. Parent-offspring pairs primarily inform estimates of relative reproductive output, while half-sibling pairs allow us to estimate total mortality. We can then partition estimates of total mortality (Z) into natural mortality (M) and fishing mortality (F) if data on catch-at-age/size are available. The application of CKMR across several years also allows us to estimate relative reproductive output by size/age and connectivity across the sampled areas.

The application of CKMR involves at least five main elements:

1. A design phase (this paper) to determine the sampling design that will yield a sufficient number of kin pairs to achieve the required level of precision in parameter estimates from CKMR. A design study evaluates the likely precision in CKMR estimates from alternative locations and size/age/sex structures of the samples;

2. Collection of tissue samples from a stratified sample of the population

3. Genotyping of the samples using a sufficient number of genetic markers that enable the detection of kin pairs;

4. Kin-finding to accurately identify kin pairs. Parent-offspring pairs (POPs), and half-sibling pairs (HSPs) have proved feasible and sufficient in applications to date. Full-sibling pairs are not useful for teleost CKMR applications;

5. A population model to find the parameters that achieve the best fit between the observed and expected number of kin pairs, given the sampling design and demographic covariates (e.g., length, age, and sex) of the population. The population model is very similar to a standard age-structured stock assessment model.

4   Methods

A CKMR design simulation model was implemented to estimate the sample sizes (of adults and juveniles) required to give reasonable precision (CV; coefficient of variation) for population metrics of interest (e.g., depletion, adult mortality, mean recruitment) for Indian Ocean yellowfin tuna.

The process consisted of four main steps, summarised here and detailed below:

i. An operating model, consisting of a simplified version of the most recent stock assessment model for yellowfin tuna (Fu et al. 2021), was produced to generate estimates of population size (in numbers) by age;

ii. The resulting equilibrium population was sampled and aged over 5 years according to the candidate sampling scenario;

iii.   The probability of observing parent-offspring-pairs (POPs) and half-sibling-pairs (HSPs) given the sampling scenario was computed, allowing us to derive the precision of key population metrics under each sampling scenario;

iv.   Alternative sampling scenarios were explored to identify sampling designs resulting in the highest precision for key population metrics.

4.1   Operating model

The operating model (OM) is a spatial, age-structured equilibrium model that replicates key features of the 2021 yellowfin tuna 'basic' assessment model (Fu et al. 2021). The model uses a quarterly timestep with an age `plus-group' of 28 quarters. The regional structure of the 'basic' assessment model (Figure 1) was retained but the 21 fisheries were simplified to retain two fisheries per region (where possible), one mostly targeting 'large' fish and one mostly targeting 'small' fish (Table 1), based on their estimated selectivities. To keep the OM as simple as possible, key quantities estimated as part of the 2021 assessment were used as fixed inputs (e.g. juvenile and adult movement matrices).
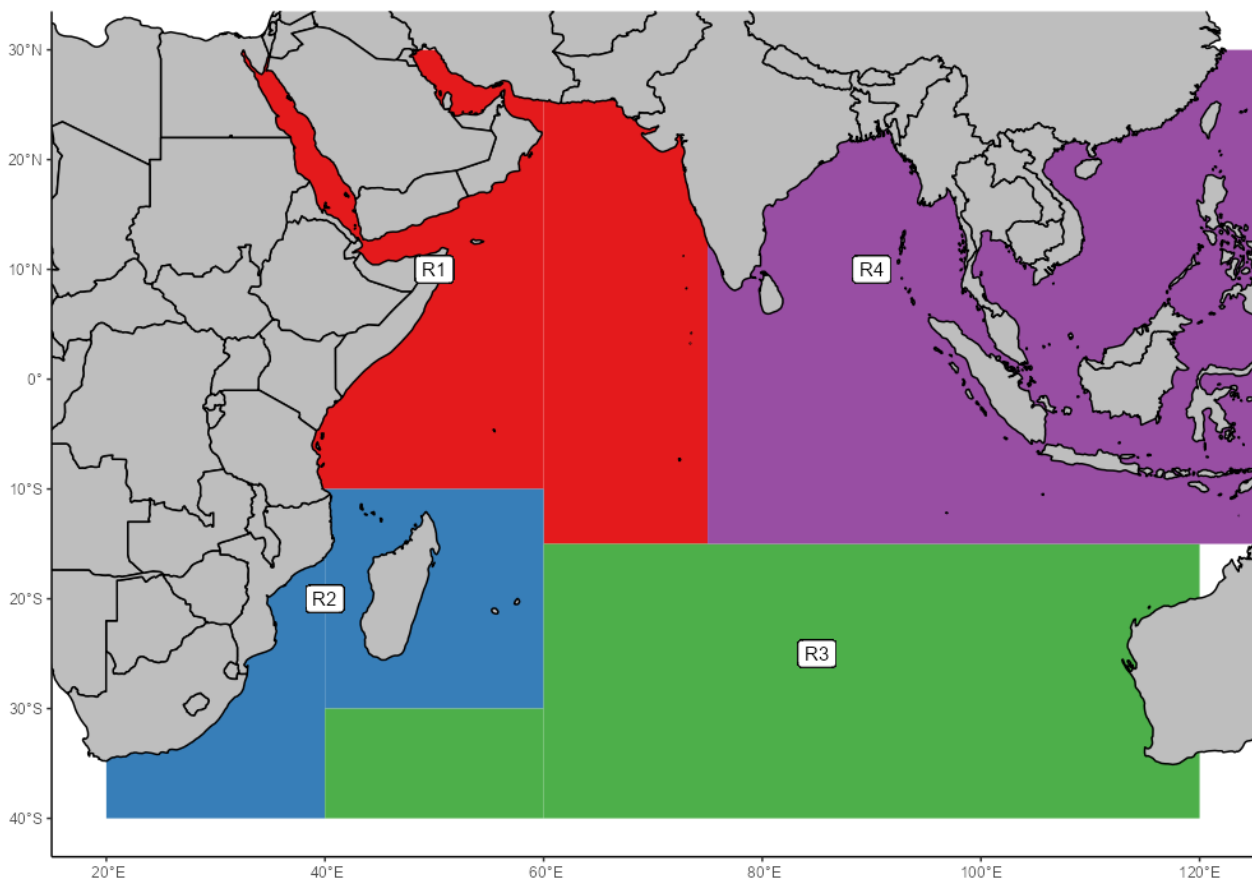

Figure 1. Four region spatial stratification of the Indian Ocean for the basic yellowfin tuna assessment model (Fu et al. 2021).

The OM was conditioned to fit (i) the overall depletion level relative to the unfished level of the 2021 assessment; and (ii) the aggregate catch biomass by fishery and region (quarterly average over the last 2 years). The parameters that were allowed to vary to meet the conditioning constraints were the overall mean recruitment and the harvest rates by fishery and region.

The population model is sexually dimorphic and uses the same life-history parameters (e.g., weight and maturity ogives, length-at-age relationship) as those of Fu et al. (2021).

Natural mortality: Adult natural mortality (M) was left as a free parameter as it is informed by close-kin probabilities. As such, M-at-age was parameterised in a slightly different way to the assessment to allow the CKMR model to inform the estimates of adult M (since close-kin probabilities are impacted by adult survival rate). Juvenile mortality was based on stock assessment values by using the maturity ogive to transition from the stock assessment's mortality-at-age vector (referred here as M_a^{juv}; Figure 14 of Fu et al. 2021) to a constant adult mortality rate:

$$M_{a,s} = M_a^{\mathrm{juv}}(1 - m_{a,s}) + M^{\mathrm{adu}} m_{a,s}$$

Assessment mortality rates in M_a^{juv} were also converted from annual to quarterly. Adult natural mortality was estimated by the model (with a starting value of M_{adu} = 0.15 qtr^{-1}). The resulting shape and magnitude of the M vector is very similar to that of the 2021 stock assessment. Estimates of M were assumed to be the same for male and females across ages.

Productivity: As this is an equilibrium model, recruitment is defined by a mean (exploited equilibrium) recruitment parameter with stochastic recruitment based on σR. σR was derived from the recruitment deviates estimated in the 2021 stock assessment. Recruitment was distributed across regions similarly to the basic assessment, but allowing more recruitment in region 2 and some recruitment in region 3 (the temperate regions).

The Total Reproductive Output (TRO) of the mature population in each time period is also computed. This metric replaces Spawning Stock Biomass in CKMR models (which itself is really a proxy for TRO), and is the main focus of the abundance-related part of the design analysis:

$$TRO_{t,s} = \sum_{a=0}^{A} N_{t,a,s} \varphi_{a,s}$$

TRO is a function of population at age and $\varphi_{a,s}$, the per capita reproductive output-at-age relative to the age class with the largest reproductive output (see Appendix I). TRO can be aggregated across space when there is an adult population in a given region, and their reproductive output (initially) belongs to that region.

Movement: Juvenile and adult movement matrices estimated by Fu et al. (2021) were used as fixed parameters to construct the overall spatial transition matrix-at-age, $\Phi_{r',r,a}$. The recent mean spatial recruitment fractions from the assessment were also used as fixed parameters. Stochastic variation in overall recruitment is estimated from the overall stock assessment deviates themselves to approximate σR; the spatial deviates are normalised to sum to 1, and we assume a variance of σ_ξ = 0.1 on the transformed scale for the random effects.

Fishing fleets and selectivities: Each of the 21 fisheries of the 2021 assessment were re-assigned to a 'small' or 'large' fishery per region based on the age (or size) distribution of their catch, except for region 3 where no fishery for small individuals exist (Table 1). Catch for the resulting 7 fisheries were aggregated from the catch of each of the component fleets (Figure 2).

Selectivity-at-age relationships for the seven fishing fleets were derived from the assessment by catch-weighting the base case estimates of the selectivity relationship of each of the component fleets and normalising the resulting relationship to a maximum value of 1 (Figure 3). Fishing fleets with size-based selectivity were first converted to mean-age-based selectivity by using the length-at-age relationship from the 2021 assessment.

Table 1. Classification of fisheries from the 2021 stock assessment into fisheries used within the CKMR operating model ('CKMR fishery').

2021 Fishery	Gear	CKMR region	CKMR fishery
GI1A	Gillnet	1	Small
HD1A	Handline	1	Large
LL1A	Longline (distant water)	1	Large
OT1A	Other	1	Small
BB1B	Baitboat	1	Small
PSFS1B	Purse seine, school sets	1	Large
LL1B	Longline (distant water)	1	Large
PSLS1B	Purse seine, log/FAD sets	1	Small
TR1B	Troll	1	Small
LL2	Longline (distant water)	2	Large
LL3	Longline (distant water)	3	Large
GI4	Gillnet	4	Small
LL4	Longline (distant water)	4	Large
OT4	Other	4	Small
TR4	Troll	4	Small
PSFS2	Purse seine, school sets	2	Large
PSLS2	Purse seine, log/FAD sets	2	Small
TR2	Troll	2	Small
PSFS4	Purse seine, school sets	4	Large
PSLS4	Purse seine, log/FAD sets	4	Small
LF4	Longline (fresh tuna)	4	Large
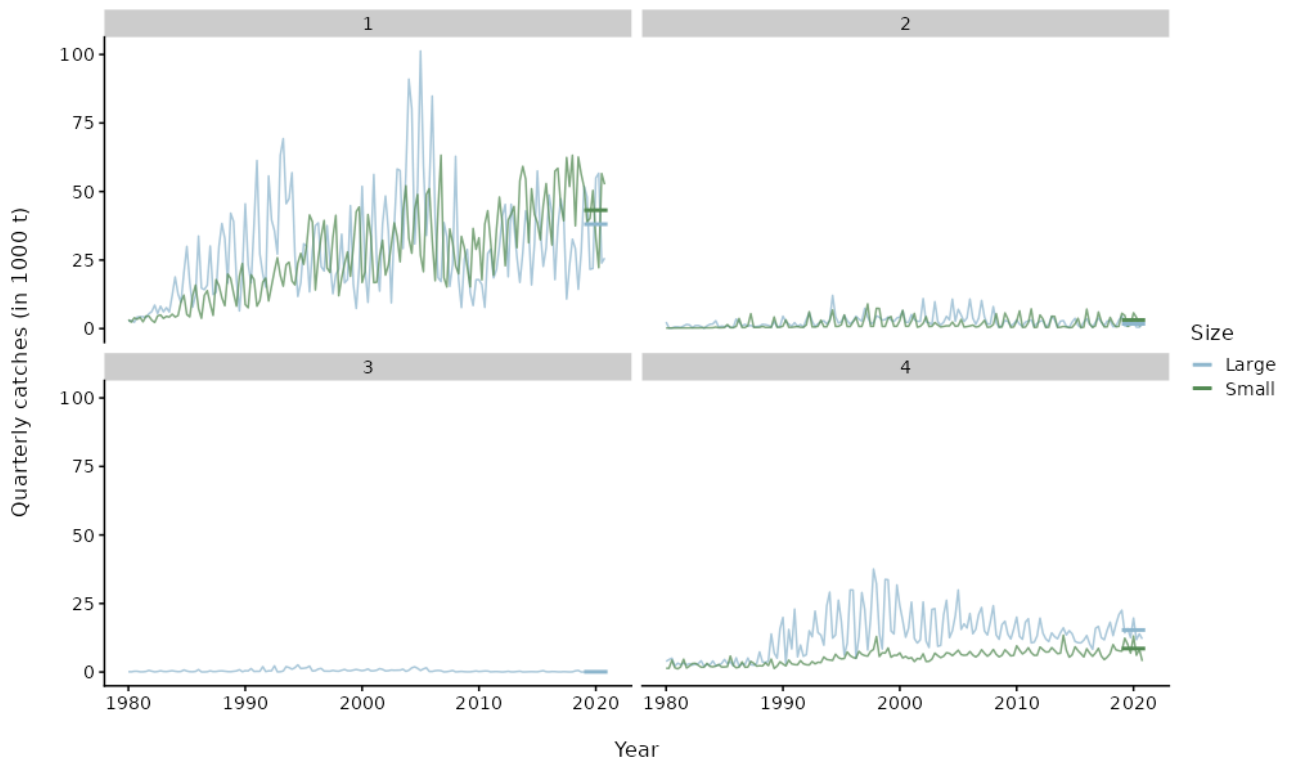
Figure 2. Figure 2. Quarterly yellowfin tuna catches per fleet (coloured lines) and region (panels). The horizontal line denotes the equilibrium catch level used to tune the operating model.
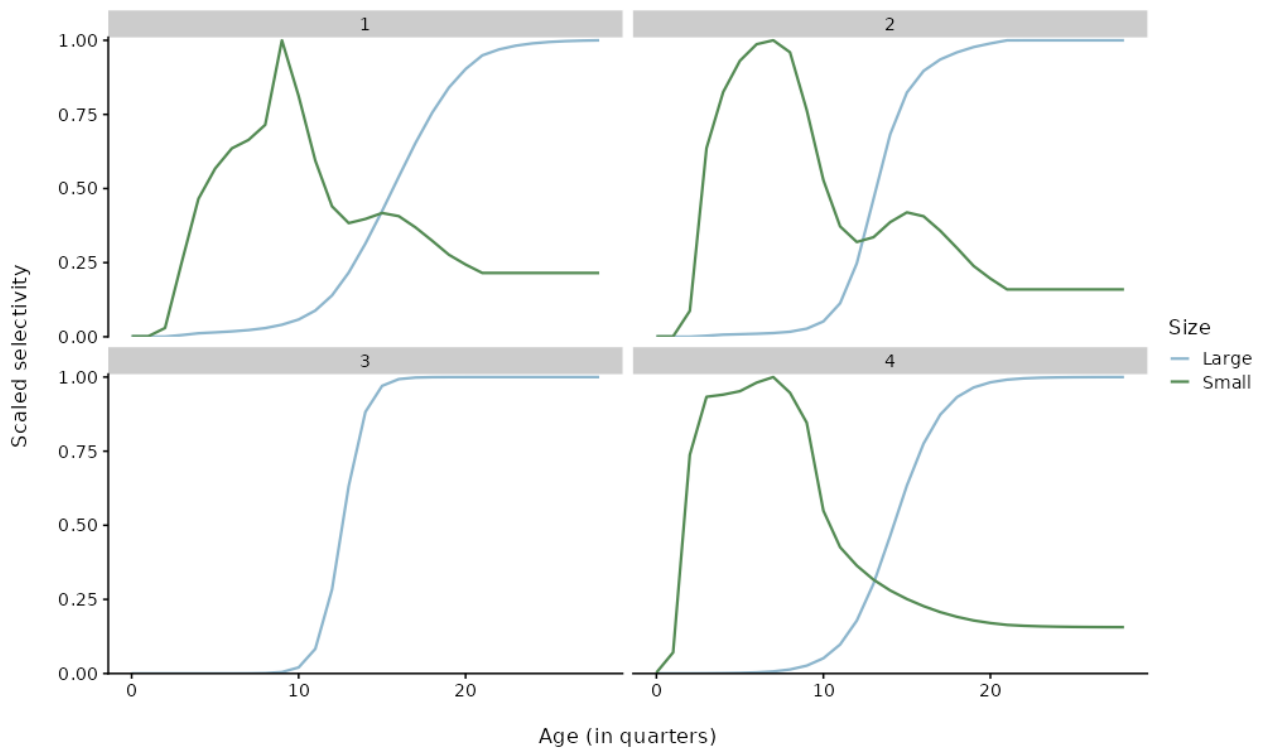

Figure 3. Age-based selectivity of the seven fleets (coloured lines) used in the operating model by region (panel). Fleets were defined based on whether they mostly catch large or small individuals. There is no 'Small' fleet in region 3.

OM conditioning: The `basic' case assessment model estimates a current depletion level of around 30% of unfished equilibrium levels. This was used as the primary conditioning target, together with the overall catch (in metric kilo tonnes; kt) of each of the small and large fleets.

The convergence criteria applied when conditioning the OM were defined so that depletion was estimated within 0.1% of the target, and overall catch biomass by fishery was estimated within 0.2% of the target.

The estimate of current overall spawning biomass was around 1,100 kt with an implied SSB_0 of around 3,600 kt. The estimates are close to the `basic' case of the assessment which predicts a current overall SSB of about 1,000 kt and an SSB_0 of about 3,300 kt (Figure 29 in Fu et al. 2021).

4.2 Estimating the sampling distribution (by sex and aggregated)

In order to compute the expected number of POPs and HSPs that will be detected for a given sampling scenario, we need to estimate the numbers-at-age of adult and juvenile sampled for each scenario.

The population was first projected over 28 quarterly time-steps assuming equilibrium total catch levels based on the quarterly average for the last two years of fishing included in the `basic' case assessment model, and equilibrium harvest rates as described earlier. The recruitment deviates are parameters of the CKMR OM.

For adults, the distribution of samples-at-age was defined to be proportional to catch-at-age, with the assumption that all adult samples come from the 'large' fleets. Region-specific selectivities were applied to generate the proportional samples-at-age, scaled to match the proportion of exploitable biomass in each region.

Juveniles were drawn from the youngest animals caught (so that movement from their natal region is minimal), and assumed to be about 3 quarters-old. For the spatially homogeneous CKMR case (see below), no regional structure was assumed when generating the juvenile samples.

4.3 Precision of management parameters under a given sampling regime

A CKMR model was developed for the spatially homogeneous case that also accounted for possible ageing error in the adult individuals sampled. For the spatially homogenous case, the adults from all regions spawn the new cohort of juveniles; the spatial regions do not act as localised reproductive units. Note that this basically replicates the current assumption in the assessment model (i.e., there is a single population of adults that produces recruits which are then distributed across all regions).

The probability that adult i and juvenile j are a parent-offspring pair was computed for each pairwise combination of adults sampled in quarter t_i with observed age at sampling a_i and sex s_i, and juvenile sampled in quarter c_j:

$$\mathbb{P}\left(POP \,|\, \{i,j\}\right) = \sum_{\tilde{a}} \left(\mathbb{I}(c_j < t_i < c_j + \tilde{a}) \frac{A_{a_i,\tilde{a}} \varphi_{\tilde{a}-(t_i-c_j),s_i}}{TRO_{c_j,s_i}} \right)$$

where $\tilde{a}$ is the true age given the observed age a_i, A is the ageing error matrix, and $\varphi_{\tilde{a}-(t_i-c_i)}$ is the proportion of the total reproductive output contributed by an individual of true age $\tilde{a}$ and sex s_i in the quarter when the juvenile was born. The identity bracket ensures that the probability outcome is zero if the adult was caught before the juvenile was born or born after the juvenile's birth quarter (see Appendix I).

The probability of two juveniles being a half-sibling pair (HSP) was computed for each pairwise combination of juvenile sampling quarters. This probability differs from that for POPs in that we never directly observe the possible shared parent; we make inferences about its dynamics from the fact that we have detected two of its offspring. For the spatially homogenous reproduction case, there are three requirements when constructing the HSP probability:

1. At the time of birth of the older juvenile, we need to account for the possible sex and age distribution of adults that could have been the individual's parent at that time;

2. We need to account for the mortality (natural and fishing related) the potential parent could have experienced between the times of birth of the older and younger juveniles being compared;

3. At the time of birth of the younger juvenile we need to calculate the probability that, of all the animals that could have been a parent of the older juvenile, the parent of the older juvenile was also the parent of the younger juvenile;

We assume that there is no ageing error when sampling juveniles because their size is representative of their age.

The probability that two juveniles from cohorts c_i and $c_{i'}$ share a parent of unknown sex and age is thus:

$$\mathbb{P}\left(HSP\,|\,\{i,i'\}\right) = \sum_s \sum_a \left(\frac{N_{c_i,a,s}\varphi_{a,s}}{TRO_{c_i,s}} \times \left[\frac{\eta_{a+\delta_i,s} N_{c_{i'},a+\delta_i,s}}{N_{c_i,a,s}} \right] \times \frac{\varphi_{a+\delta_i,s}}{TRO_{c_{i'},s}} \right)$$

In order to ensure that juvenile comparisons are between individuals belonging to two different cohorts, comparisons are only made for juvenile samples separated by at least 6 months. We also assumed that all HSPs could be correctly identified using genetic methods (i.e. the rate of false negatives is 0).

In order to generate variance estimates for estimated population variables, a Hessian matrix is constructed for the key estimable parameters via an approximation to the Fisher information matrix constructed by summing the information from each set of pairwise CKMR comparison (Appendix I). The Fisher information is a metric of information content commonly used in mathematical statistics.

From the Hessian, approximate estimates of the variance of derived population quantities (e.g., TRO, mean recruitment level) can then be obtained from the delta method. Automatic differentiation via the TMB package in R (Kristensen et al. 2016) is used so that all gradients and derived quantities are calculated to machine precision. The full process is detailed in Appendix I.

A spatially heterogenous CKMR design was also developed (see Appendix I), with individual age assumed to be known exactly. Preliminary results are included for comparison with the spatially homogeneous case.

4.4   Sampling scenarios

Two axes of sampling scenarios were defined: in the first one, the overall number of annual samples was varied in increments of 5,000 from 20,000 to 60,000. In the second scenario axis, the proportion of juveniles in the annual samples varied from 0.1 to 0.9 in increments of 0.1.

For the spatially heterogenous case, the first axis of sampling scenarios (i.e., total sample size) was tested with a proportion of 50% adults in the annual samples.

5   Results

The expected number of kin pairs were estimated based on each sampling scenario (Figure 4), and the coefficients of variation were computed for the resulting mean recruitment, adult natural mortality, depletion in total reproductive output and overall total reproductive output (Figure 5).
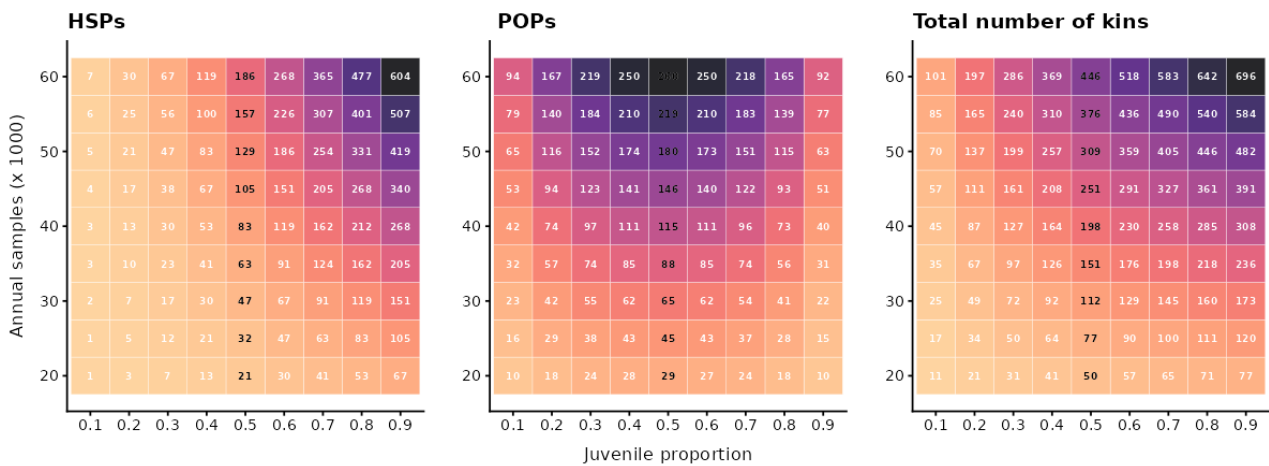

Figure 4. Expected number of kin pairs (numbers in cells) by kin type (panels) detected along the two axes of sampling scenarios: increasing proportion of juveniles in the sample (X-axis) and annual number of samples (Y-axis). Numbers in bold highlight the scenarios with equal proportion of adults and juveniles.

A general rule of thumb for CKMR studies is that at least 50 to 100 kin pairs are required to generate useful estimates of population metrics. In addition, as POPs and HSPs give insights on different population parameters, this number should be spread across the two kin types (based on management priorities; see Discussion). For this design study, the total number of detected kin pairs increased, as expected, with annual sample numbers (Figure 4). There were also more kin pairs detected for the same sample number when the proportion of juveniles in the samples was lower, although with fewer POPs. At annual sampling levels of 25,000 and 30,000 individuals, 77 and 112 kin pairs were detected, respectively, when equal proportions of juveniles and adults were sampled.

Different levels of precision were achieved for each of the four focal population metrics, with highest precision achieved for depletion in total reproductive output across all sampling scenarios (Figure 5). For this metric, CVs of 15.3% and 12.9% were predicted under annual sampling levels of

25,000 and 30,000 individuals, with additional improvement in CVs with a higher proportion of juveniles in the sample (e.g. CVs of 13.0% and 11.1% with 70% juveniles in the annual samples of 25,000 and 30,000).

Given 30,000 annual samples spread evenly over adults and juveniles, CVs of 32.9%, 26.5% and 21.8% were achieved for mean recruitment levels, adult mortality and total reproductive output (Figure 5).
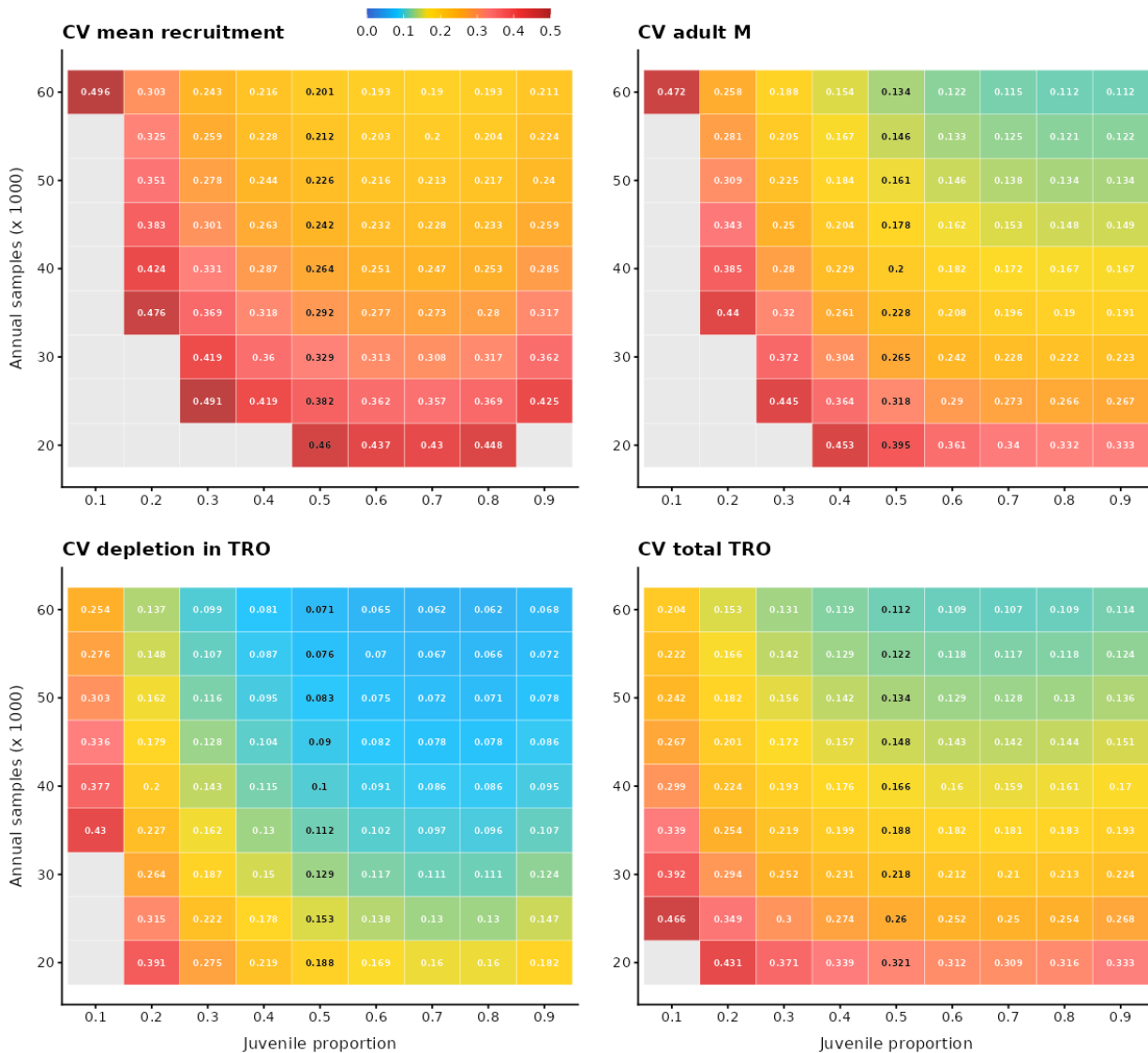

Figure 5. Coefficients of variation (CVs) for four population metrics under two axes of sampling scenarios: increasing proportion of adults in the sample (X-axis) and annual number of samples (Y-axis). Numbers in bold highlight the scenarios with equal proportion of adults and juveniles, with the size of the CV depicted by the coloured gradient; cells in grey have CV > 0.5.

The main simulation results assumed no spatial structure when computing kin probabilities. A preliminary model accounting for movement between the region where an individual had spawned vs. where it was captured showed little to no inflation in CV resulting from the inclusion of movement (Figure 6). As the current version of the spatial model was derived assuming exact age, we also include CVs from an earlier version of the close-kin spatially homogeneous model assuming exact age for comparison.
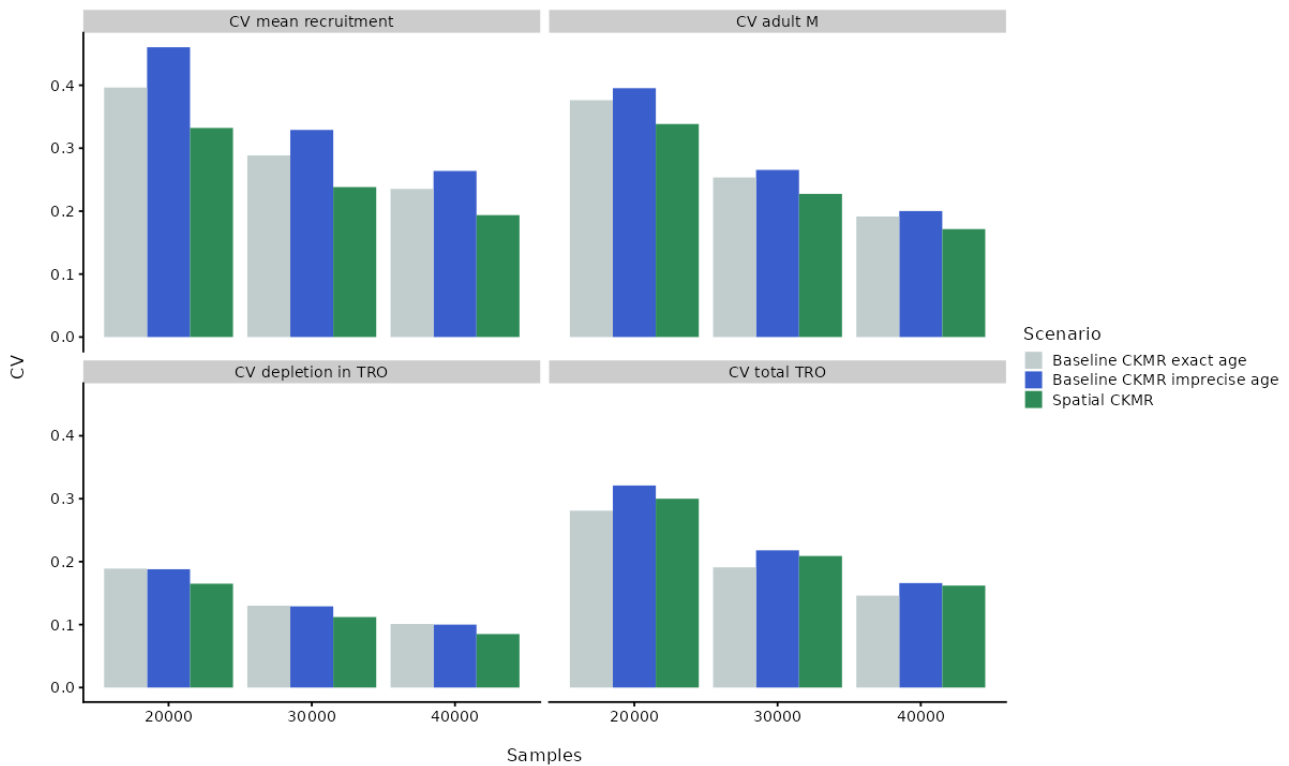
Figure 6. Comparison of coefficients of variation (CV) for key management metric (panels) under three phases of development for the CKMR model (coloured bars). The spatial version of the model shows preliminary results. Scenarios use an even distribution of adults and juveniles in the samples.

6 Sampling design considerations

CKMR requires the collection of uncontaminated tissue samples from a mix of size classes across time and space. The fleets and fisheries that will most likely be of utility in undertaking large-scale sampling programs for the purposes of CKMR, are those currently providing length data. Getting an adequate spread of samples across time and space will be important to account for any population structuring, movement, and spatial variation relevant to stock parameters (e.g., mortality). A mix of size classes of yellowfin tuna will also be required to ensure that both potential offspring and parents are adequately sampled. The juveniles samples will need to be young enough to infer their region of spawning.

To evaluate the potential to collect sufficient samples of yellowfin tuna for CKMR, we examined length data reported to the IOTC in each of the four stock assessment regions (Figure 1), with the assumption that collecting tissue samples from fish that are already measured is likely to be easier than establishing supplementary sampling programs. Within each of the four regions, length data were separated into two main size classes (<50 cm FL and >75 cm FL) to represent the juvenile and adult samples to be sampled for CKMR.

There are two strong modes in the length frequency data (Figure 7) that reflect the difference in targeting and selectivity of gear types, and the distribution of juvenile yellowfin tuna (Fu et al. 2021). Longline and free school purse seine sets generally catch yellowfin tuna greater than 75cm, while log/FAD set purse seine and bait boats generally catch yellowfin tuna less than 50cm (Figure 8). Most length data have been reported from Region 1 and Region 4 and these are also the main

regions where large numbers of small yellowfin tuna (<50cm) are reported. This is to be expected as yellowfin tuna spawn in tropical, equatorial waters and juveniles are less common in more temperate waters (Zudaire et al. 2013). Large yellowfin tuna (>75cm) are routinely reported in all regions except for Region 3 where sampling is relatively sparse due to substantially reduced fishing effort in this region.
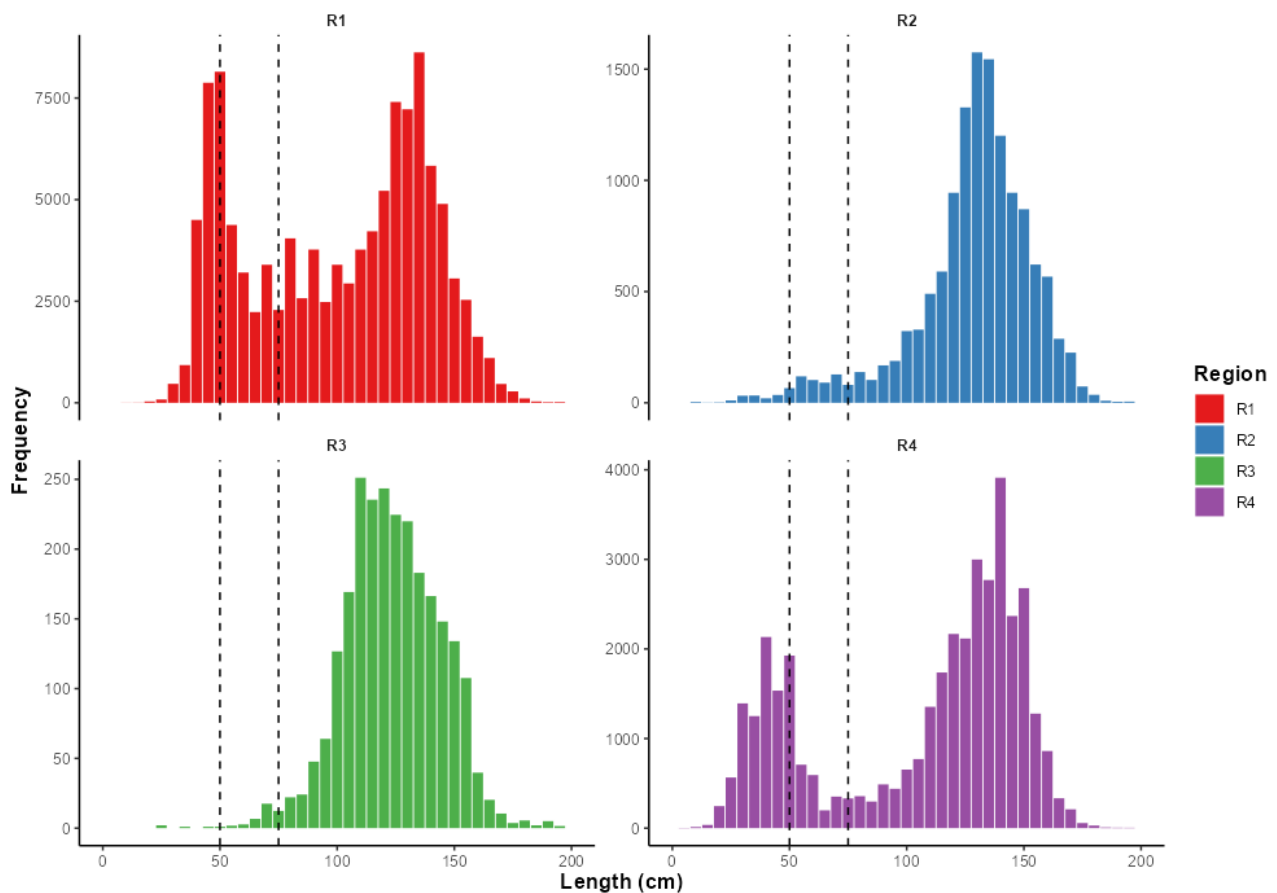

Figure 7. Average annual length frequency distribution of sampled Indian Ocean yellowfin tuna by region (panels) from 2010-2020 with two vertical dashed lines denoting potential offspring (<50cm) and parents (>75cm). Note independent y-axes.

Results from the CKMR design simulation suggest that approximately 30,000 samples of yellowfin tuna per year over five years (150,000 samples in total) would be required to achieve adequate recaptures of kin pairs to provide acceptable levels of precision for key population metrics. Based on Figure 5, a sampling regime of 70% offspring and 30% adults provides optimal results in terms of precision. Given this information, and if uniform sampling was assumed across the four regions and two size classes, this would require around 2,250 large yellowfin tuna (>75cm) sampled each year from each region, and 10,500 small yellowfin tuna (<50cm) from Region 1 and Region 4 (as very few juveniles are likely to be sampled from Region 2 and Region 3).
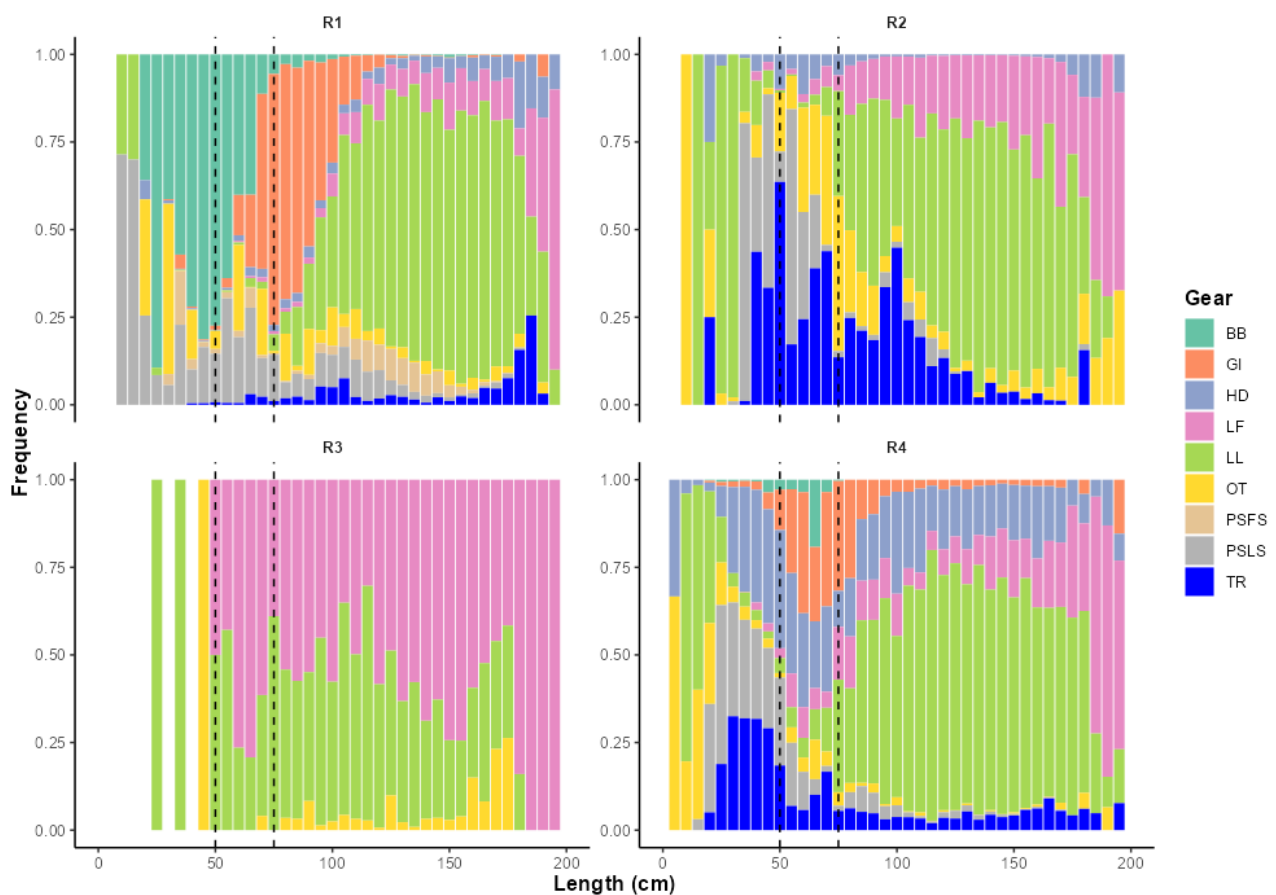
Figure 8. Average annual length frequency distribution of yellowfin tuna by fishery in the Indian Ocean from 2010-2020 by region (panels) and gear (colour). Vertical dashed lines denoting potential offspring (<50cm) and parents (>75cm). BB = Bait boat. GI = Gillnet. HD = Handline. LF = Longline fresh. LL = Longline. OT = Other. PSFS = Purse seine free set. PSLS = Purse seine log set. TR = Troll.

This level of sampling intensity is already achieved across most region and size class combinations in the length data collection programs currently implemented by IOTC member countries (Figures 9 & 10). For small yellowfin tuna (<50cm), more than 10,000 individuals have been sampled on average in Region 1 and Region 4 each year from 2010-2020 (Figure 9). In Region 1, >10,000 samples are taken from the bait boat fishery alone. However, in Region 4 length samples are more evenly dispersed across gear types and may require a more comprehensive sampling program to collect adequate numbers. For large yellowfin tuna (>75cm), more than 2,000 individuals have been sampled annually on average from 2010-2020 across all regions, although the sampling intensity in Region 3 is much lower than other regions (Figure 10). An informed and substantial sampling program will be required to collect this number of samples across regions and size classes throughout the Indian Ocean. This will require collaboration and cooperation from numerous member nations, institutes, organisations and most importantly fishers, observers, and port samplers.

Figure 9. Top three fisheries that provide length samples of small yellowfin tuna (<50 cm) by region in the Indian Ocean and the average number of samples they have provided per year by gear type from 2010-2020. BB = Baitboat. HD = Handline. LL = Longline. PSLS = Purse seine log set. OT = Other. TR = Troll.
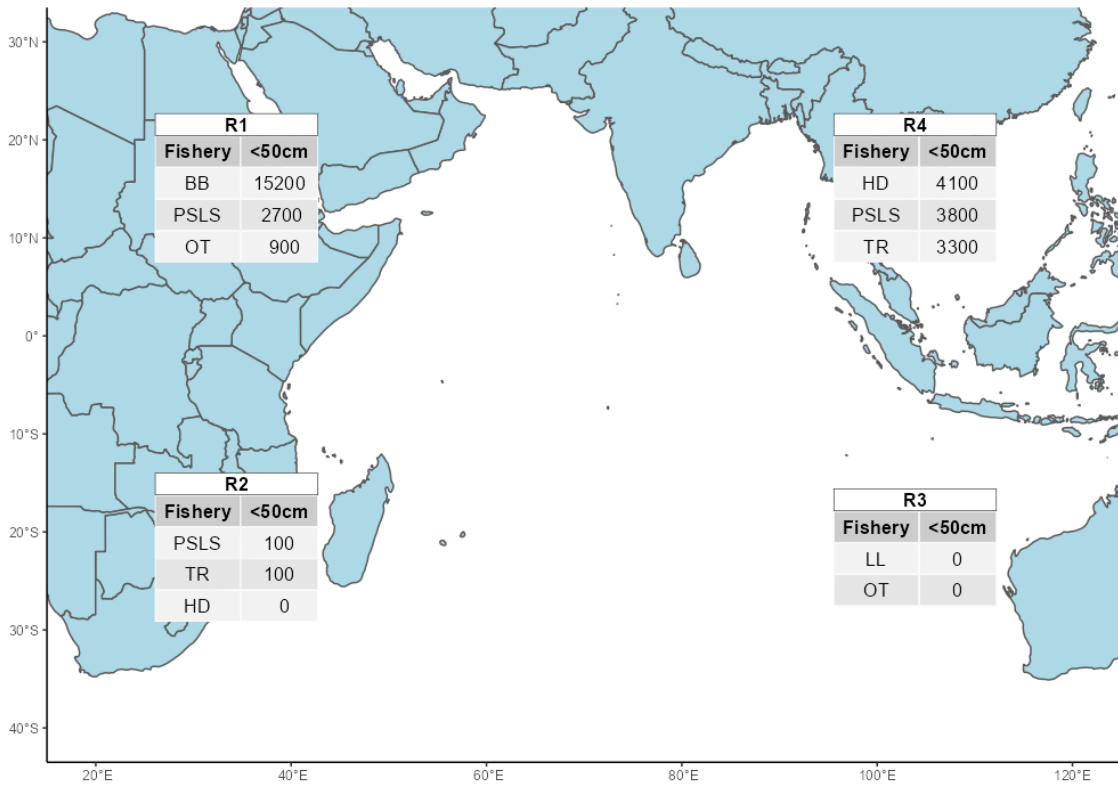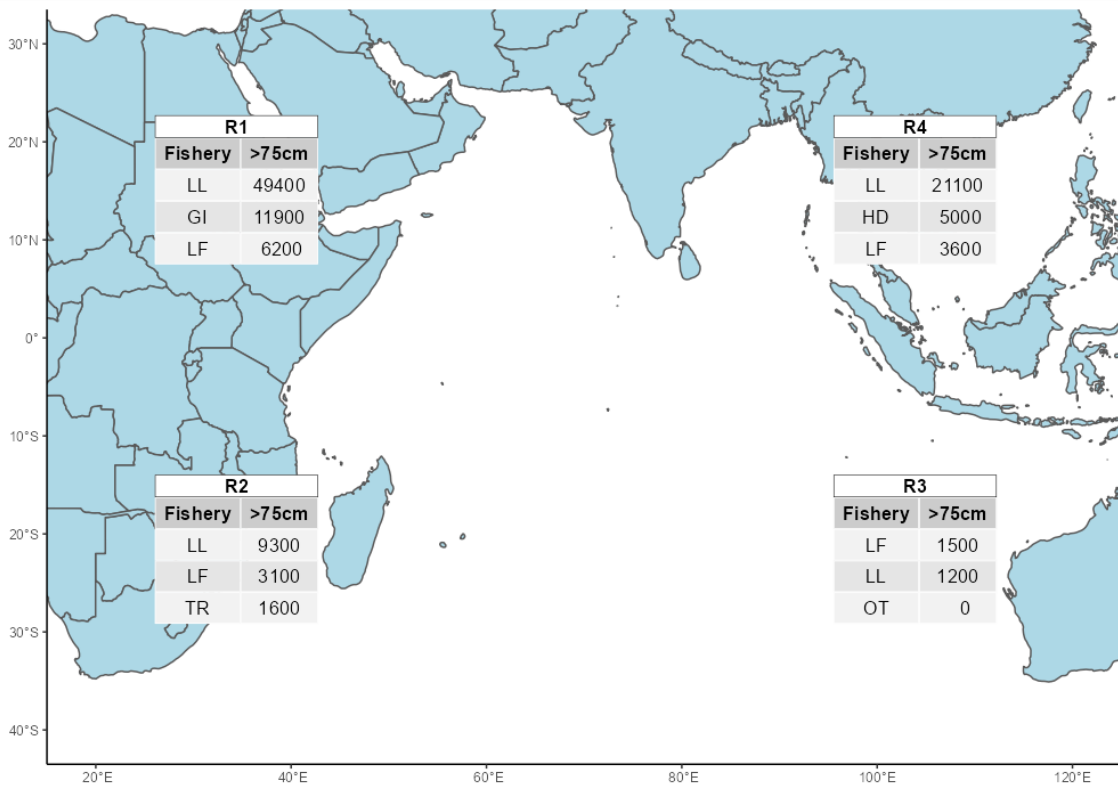

Figure 10. Top three fisheries that provide length samples of large yellowfin tuna (>75 cm) by region in the Indian Ocean and the average number of samples they have collected per year by gear type from 2010-2020. GI = Gillnet. HD = Handline. LL = Longline. LF = Longline fresh. OT = Other. TR = Troll.

7   Discussion

This report evaluates a range of sampling scenarios designed to estimate key population metrics of Indian Ocean yellowfin tuna using CKMR. The analysis used a simplified population model that reproduced recent yellowfin tuna population dynamics, but in an equilibrium framework. Under these conditions, annual sampling levels of 25,000 to 30,000 samples were predicted to yield informative insights on population metrics based on the resulting precision in these estimates. Specifically, the depletion in total reproductive output (TRO), a metric with a similar interpretation to the depletion in spawning stock biomass, could be estimated with a CV of 15% given 30,000 annual samples after 5 years.

CKMR approaches allow us to gain insights on population parameters that were previously hard to estimate using conventional methods, such as adult natural mortality rates. While precision in adult M is not as high as for depletion in TRO, improvement in the precision of this quantity can be achieved by collecting a higher proportion of juveniles. This is because more HSPs are expected to be detected with higher proportions of juveniles sampled, and half-sibling probabilities are impacted by adult survival rates. For instance, by decreasing the proportion of adults sampled to 30% (i.e., 70% juvenile samples), we can improve the precision in CV of adult M by about 4 points.

Collecting a higher proportion of juveniles as part of the annual samples is also practical from a sampling logistics perspective, because more juveniles (<50 cm) than adults (>75 cm) are currently measured as part of existing length frequency sampling programs in the IOTC, and it will be easier to collect genetic samples from these fish than to implement supplementary sampling programs. There is no loss in the precision of management quantity estimates as long as at least 20-30% of the annual samples are taken from adults.

Of note, even if population dynamics based on the 2021 stock assessment are not representative of true population status, CKMR would still yield useful information. If fewer kin pairs are detected than expected, it implies that absolute levels of population abundance are higher than those predicted by the 2021 stock assessment (used for the simulation). Conversely, if more kin pairs are detected than expected, absolute levels of population abundance are lower than those predicted by the 2021 stock assessment, but CKMR-based estimates of population abundance will be more precise. In addition, new insights about stock structure would be achieved by looking at the spatial distribution of detected kin pairs (e.g., see Trenkel et al. 2022).

The application of CKMR requires an estimate of age for the individuals that are sampled to determine birth year and age-specific parameters for the calculation of kinship probabilities. While we can predict the age of juvenile yellowfin tuna (<50 cm) from length with reasonable precision, estimating the age of adult yellowfin tuna from length is more problematic, due to large variation in size-at-age and asymptotic growth (Farley et al. 2021). Otoliths currently provide the most reliable estimates of age for tunas, but it is unlikely that sufficient otoliths could be collected, processed and analysed each year for adult yellowfin tuna. Recent advances in epigenetic ageing using DNA methylation have demonstrated encouraging results across a range of species (Mayne et al. 2020, 2021). This would present a more viable option for CKMR sampling of yellowfin tuna as the same tissue sample could be used for both genotyping and epigenetic ageing. The results from this CKMR simulation are robust to potential ageing error from epigenetic ageing because the ageing error we applied in our CKMR model (CV=0.15 across ages) approximates the ageing error

observed in epigenetic ageing for other species. Of note, sex can also be obtained from the DNA sample, which negates the need to collect gonad tissue and reduces the potential error associated with macroscopic determination of sex by observers.

We arbitrarily chose a program length of 5 years for this analysis as a reasonable starting point for a sampling program. Other timelines could also be explored. Of note, once a CKMR sampling program has been established (i.e., it achieves satisfactory CVs for population parameters of interest), ongoing sampling can proceed at lower intensity while continuing to yield updated estimates of similar (or better) precision. This is because, within reasonable time frames, the pool of possible kin comparisons grows exponentially with the number of samples.

The next steps in the development of the CKMR methodology for Indian Ocean yellowfin tuna will include finalising the spatial CKMR model to account for imprecise age, explorations of spatial scenarios refining juvenile sampling and ageing given the distribution of juvenile-targeting fisheries and the current understanding of juvenile movement. In addition, inclusion of adult samples in half-sibling probability computations could be considered, however these would be complicated by the need to account for movement by both potential sibling and their potential parent. As such, development of adult HSP probabilities is likely to remain a low priority.

While developments to the CKMR model for Indian Ocean yellowfin tuna are ongoing, we deem the current version sufficient to inform discussions by the Working Party on Methods, Working Party on Tropical Tuna, and the Scientific Committee with regards to the implementation and logistics of a CKMR sampling program for yellowfin tuna.

8 References

Bravington, M.V., Skaug, H.J., Anderson, E.C. 2016. Close-Kin Mark-Recapture. *Statistical Science* 2016, Vol. 31(2), 259–274.

Farley, J., Krusic-Golub, K., Eveson, P., Luque, P.L., Clear, N., Fraile, I., Artetxe-Arrate, I., Zudaire. I., Vidot, A., Govinden, R., Ebrahim, A., Ahusan, M., Romanov, E., Shahid, U., Chassot, E., Bodin, N., Parker, D., Murua, H., Marsac, F., Merino, G. 2021. Estimating the age and growth of yellowfin tuna (*Thunnus albacares*) in the Indian Ocean from counts of daily and annual increments in otoliths. Working paper IOTC-2021-WPTT23-05_Rev1 presented to the 23rd Working Party on Tropical Tuna.

Fu, D., Ijurco, A.U., Cardinale, M., Methot, R., Hoyle, S. & Merino, M. 2021. Preliminary Indian Ocean yellowfin tuna stock assessment 1950-2020 (Stock Synthesis). Working paper IOTC–2021–WPTT23–12 presented to the 23rd Working Party on Tropical Tuna.

Hillary, R., Preece, A., & Davies, C. 2019. Performance of a revised candidate MP using all 3 input data sources. Paper CCSBT-ESC/1909/16 prepared for the Extended Scientific Committee for the Twenty Fourth Meeting of the Scientific Committee. Commission for the Conservation of Southern Bluefin Tuna.

Hillary, R., Preece, A., & Davies, C. 2020. Summary of updated CKMR data and model performance in the Cape Town Procedure. Paper CCSBT-ESC/2008/BGD 07 prepared for the Extended Scientific Committee for the Twenty Fifth Meeting of the Scientific Committee. Commission for the Conservation of Southern Bluefin Tuna.

IOTC 2017. Report of the 20th Session of the IOTC Scientific Committee. 30 November – 4 December 2017. IOTC–2017–SC20–R[E], Seychelles.

IOTC 2021. Report of the 24th Session of the IOTC Scientific Committee Held by video-conference, 6 – 10 December 2021. IOTC–2021–SC24–R[E]_Rev1.

Kolody, D., Bravington, M. 2019. Is Close-Kin Mark Recapture feasible for IOTC Yellowfin Tuna Stock Assessment? IOTC–2019–WPM10–25-rev.1 Prepared for the Indian Ocean Tuna Commission Working Party on Methods and Working Party on Tropical Tunas, San Sebastien.

Kristensen, K., Nielsen, A., Berg, C.W., Skaug, H. & Bell, B.M. 2016. TMB: Automatic Differentiation and Laplace Approximation. *Journal of Statistical Software*, 70(5), 1–21.

Mayne, B., Korbie, D., Kenchington, L., Ezzy, B., Berry, O. & Jarman, S. 2020. A DNA methylation age predictor for zebrafish. *Aging* (Albany NY), 12(24), 24817.

Mayne, B., Espinoza, T., Roberts, D., Butler, G.L., Brooks, S., Korbie, D. & Jarman, S. 2021. Nonlethal age estimation of three threatened fish species using DNA methylation: Australian lungfish, Murray cod and Mary River cod. *Molecular Ecology Resources*, 21(7), 2324-2332.

Trenkel, V. M., Charrier, G., Lorance, P. & Bravington, M.V. 2022. Close-kin mark–recapture abundance estimation: practical insights and lessons learned. *ICES Journal of Marine Science*, 79(2), 413-422.

Zudaire, I., Murua, H., Grande, M. & Bodin, N. 2013. Reproductive potential of yellowfin tuna (*Thunnus albacares*) in the western Indian Ocean. *Fishery Bulletin*, 111, 252–264.

Appendix I

This section provides supplementary information detailing:

1. The construction of the relevant CKMR kin probabilities for the spatially homogeneous and the spatially-structured case;

2. The technical derivation of the approach used to translate the CKMR kin probabilities into a parameter covariance matrix to generate approximate uncertainty estimates of key population dynamics variables.

Key parameters of the operating model

The CKMR design process uses a pre-specified set of estimable model parameters, $\boldsymbol{\theta}$, and the theory behind the concept of the Fisher information (see below), to derived approximate uncertainty estimates in key model outputs (e.g. adult abundance and mortality) for a given sampling strategy. The set of possible model parameters we explore is restricted to ones that we would expect the CKMR data to be informative on:

- Overall abundance scaling parameter (mean recruitment)

- Reproductive output-at-age in adults

- Adult movement patterns (for spatial reproductive structure)

To define the adult population, for each sex, we use a generalisation of the spawning stock biomass concept:

$$\varphi_{a,s} = \frac{m_{a,s} w_{a,s}^{\psi_s}}{\max_i \{m_{i,s} w_{i,s}^{\psi_s}\}}$$

This functional relationship was initially defined for Southern Bluefin tuna (SBT) where the assessment includes both POPs and HSPs. The parameters ψ_s (which *could* differ by sex) define the degree to which the concept of SSB needs to be generalised to accommodate the **realised** per capita output of each age class. Values of $\psi_s = 1$ coincide with the SSB; values greater than 1 (e.g. for SBT they are closer to 2) mean older, heavier animals contribute more to the production of newborn animals than would be assumed to be true in the SSB paradigm. The age structure of the POPs in particular, but also the ratio of POPs to HSPs, are the main informative CKMR data on these parameters. It is sensible to normalise somehow these numbers when using a power parameter approach such as this. We normalise to the maximum across all ages which leads to

the following interpretation for $\varphi_{a,s}$: the *per capita* reproductive output-at-age relative to the age class with the largest reproductive output. This then leads to the concept of the Total Reproductive Output (TRO) as the key variable of overall adult population "size":

$$TRO_{t,s} = \sum_{a=0}^{A} N_{t,a,s}\varphi_{a,s}$$

This replaces the SSB (itself a proxy for TRO), and is the main focus of the abundance-related part of the design analysis. It also generalises spatially when we have an adult population in a given region and their reproductive output (initially) belongs to that region. For recruitment we account for the stochastic variability in both overall and spatial relative recruitment by using the empirical variation from the assessment to define σ_R and an assumed value of $\sigma_\xi = 0.1$ for the generalised-logit transformed spatial recruitment variates. This ensures that we are being more precautionary in our estimates of uncertainty by implicitly including this variability in the calculations. For the spatially stratified reproduction case we must expand our parameter vector to include the parameters required to define adult movement between regions: Φ^{adu}. We use juvenile and adult movement matrices from the 2021 stock assessment (Fu et al. 2021) with the following parameterisation to achieve an overall age specific spatial transition matrix:

$$\Phi_{r',r,a} = \Phi_{r',r}^{\mathrm{juv}}(1 - \bar{m}_a) + \Phi_{r',r}^{\mathrm{adu}}\bar{m}_a,$$

and $\bar{m}_a$ is the sexually-averaged maturity-at-age. For R spatial regions, the transition matrix is an $R \times R$ matrix whose rows sum to 1, which takes $R \times (R-1)$ free parameters to fully define. So, we get an additional 12 degrees of freedom for the spatially stratified reproductive case when we include the 4 spatial regions (Figure 1, main section) as reproductive "units".

Spatially homogeneous CKMR probabilities

The spatially homogeneous case is the simplest case explored here, where the adults across all regions give rise to the overall number of juveniles, and the spatial regions do not act as localised reproductive units. Note that this essentially replicates the current assumption in the assessment model: there is a single parental stock and it produces the total number of recruits, which are then distributed across the regions as specified.

Parent-Offspring Pairs (POPs)

The key covariates required to compute the probability that a juvenile is the offspring of a possible parent are, for the juvenile, its (known) birth cohort, c_j, and, for the adult, time t_i of sampling, age a_i at sampling, and, possibly, also its sex, s_i. Given spatially homogeneous reproduction we sum across regions to get the spatially aggregated abundance and TRO:

$$N_{t,a,s} = \sum_{r=1}^{R} N_{t,a,s,r}$$

$$TRO_{t,s} = \sum_{a=0}^{A} N_{t,a,s} \varphi_{a,s}$$

We can now define the sex-specific POP probability as follows:

$$\mathbb{P}\left(POP \,|\, \{i,j\}\right) = \mathbb{I}(c_j < t_i < c_j + a_i) \frac{\varphi_{a_i - (t_i - c_j), s_i}}{TRO_{c_j, s_i}}$$

The indicator bracket, $\mathbb{I}()$, ensures that (a) the adult was not caught *before* the juvenile was born (and, hence, could not be its parent); and (b) that it was born before the juvenile was. If the sex of the adult is unknown we simply sum the maternal and paternal POP probabilities together. Note here that we make the simplifying assumption that adults in the plus-group can be ignored when doing the comparisons.

This formulation assumes we have perfect knowledge of the age of the adult at the time of sampling; realistically, it is more likely that we will have an estimate of age (e.g., otolith, epigenetic age), not the true age. To deal with ageing error we propose to use an ageing error matrix; specifically we construct a matrix A where each row in the matrix is the probability of the true age $\tilde{a}$ given the observed age a, so that $\sum_{\tilde{a}} A_{a,\tilde{a}} = 1$. The modified POP probability is then:

$$\mathbb{P}\left(POP \,|\, \{i,j\}\right) = \sum_{\tilde{a}} \left(\mathbb{I}(c_j < t_i < c_j + \tilde{a}) \frac{A_{a_i, \tilde{a}} \varphi_{\tilde{a} - (t_i - c_j), s_i}}{TRO_{c_j, s_i}} \right)$$

For the ageing error case, we need to explicitly deal with the plus-group, as any possible parent might belong to the plus-group given ageing error. To do this we assume $\varphi_{a,s}$ to be based on the expected age in the plus group, which can be derived from the mortality parameters. This is an approximation to the full problem, which would require integrating across all ages in the plus-group.

Half-Sibling Pairs (HSPs)

Half-sibling pairs are *typically* focussed on comparisons between juveniles, i and i', to ensure as much accuracy as possible in the cohorts, c_i and $c_{i'}$, of the two animals. HSPs differ from POPs because we do not directly observe the putative shared parent; we make inferences about its characteristics (e.g., age, sex, ...) from the fact that we have detected two juveniles that share that parent. For the spatially homogenous reproduction case there are three factors to take into account of when constructing the HSP probability:

1. At the time of birth of the older juvenile, what was the possible age distribution and sex of adults that could have been its parent at that time?

2. What is the chance that the putative parent survived from the time of birth of the older juvenile to the time of birth of the younger juvenile, c_i to $c_{i'}$? This should account for both natural and fishing-related mortality.

3. At the time of birth of the younger juvenile, what is the probability that, of all the animals that could have been a parent of the older juvenile, it was in fact *the* parent of the younger juvenile?

Since we do not observe the potential parent, HSP computation integrates over all possible parent ages. As such, ageing error of adult samples is not a factor for HSPs so there is a single formulation for the HSP probability:

$$\mathbb{P}\left(HSP \,|\, \{i, i'\}\right) = \sum_s \sum_a \left(\frac{N_{c_i,a,s}\varphi_{a,s}}{TRO_{c_i,s}} \times \left[\frac{\eta_{a+\delta_i,s}N_{c_{i'},a+\delta_i,s}}{N_{c_i,a,s}} \right] \times \frac{\varphi_{a+\delta_i,s}}{TRO_{c_{i'},s}} \right),$$

where $\delta_i = c_{i'} - c_i$ is the elasped time between the birth of the two juveniles, and $\eta_{a+\delta_i,s}$ is a term to deal with the case where the age of the adult at time $c_{i'}$ is in the plus group (what fraction of the true age $a + \delta_i$ is actually in the plus group). Each of the successive fractional terms in the above equation corresponds to each of the three processes in the HSP probability as described above. Note that we assume here that juvenile age is known without error.

Spatially structured CKMR probabilities

The next level of complexity in the design modelling is to account for spatial structure in the reproductive output (and hence the CKMR probabilities). We limit the spatial CKMR work to adult movement only for this first instance of a fully developed CKMR design paper submitted to the

Scientific Committee. We do not assume to know where a sampled adult was in when the juvenile was born, but we assume that we are able to select juveniles for the sampling program at a sufficiently young size/age that we can be sure they were born within the region of sampling. If we cannot make this assumption, we need to build in additional complexity to the CKMR probabilities accounting for the probability that the juvenile was born in a natal region where the parent spawned given the regions where juvenile and possible parent were captured. We also assume that adult age is known exactly, but it is straightforward to extend the probabilities to account for ageing error as outlined above.

Parent-Offspring Pairs (POPs)

The juvenile covariates required for this computation are the birth time and region, $\{c_j, r_j\}$; for the adult covariates age, sex and region, $\{t_i, a_i, s_i, r_i\}$ are required. Given we assume to know the birth location of the juvenile, the additional factor we need to account for in the POP probability is the probability that the adult was, at the birth time of the juvenile, in the birth region of the juvenile conditional on the observation that, some time later, it was sampled in a (potentially) different region.

We thus require the following probability: $\mathbb{P}(\{c_j, \alpha_{i,j}, s_i, r_j\} \,|\, \{t_i, a_i, s_i, r_i\})$, where $\alpha_{i,j} = a_i - (t_i - c_j)$. From a Bayesian perspective, we can easily calculate the following probability: $\mathbb{P}(\{t_i, a_i, s_i, r_i\} \,|\, \{c_j, \alpha_{i,j}, s_i, r_j\})$ i.e., the probability that the adult was alive and aged a_i at time t_i and in region r_i given it was alive *etc.* at time c_j in region r_j. This probability is computed from the mortality and movement rates as follows: set the vector (of length 4, the number of spatial regions) $\mathbf{u}_0$ as a unit vector with value 1 at location r_j and zero elsewhere. For the time periods between c_j and t_i, we update this vector as follows:

$$u_{t+1,r} = \sum_{r'} u_{t,r'} \Phi_{r',r,a_t} \exp(-M_{a_t,s_i}) \left(1 - h_{a_t,r'}\right)$$

where $a_t = \alpha_{i,j} + t$ and until $t + 1 = t_i - c_j$. We can assume that there would be no prior information on the adult's state of nature at the birth time of the juvenile *before* we observed it. So, from Bayes' theorem, the probability can be computed as follows:

$$\mathbb{P}(\{c_j, \alpha_{i,j}, s_i, r_j\} \,|\, \{t_i, a_i, s_i, r_i\}) = \frac{\mathbb{P}(\{t_i, a_i, s_i, r_i\} \,|\, \{c_j, \alpha_{i,j}, s_i, r_j\})}{\sum_{r'} \mathbb{P}(\{t_i, a_i, s_i, r'\} \,|\, \{c_j, \alpha_{i,j}, s_i, r_j\})}$$

which then becomes:

$$\mathbb{P}(\{c_j, \alpha_{i,j}, s_i, r_j\} \,|\, \{t_i, a_i, s_i, r_i\}) = \frac{u_{t_i - c_j - 1, r_i}}{\sum_{r'} u_{t_i - c_j - 1, r'}}$$

The spatial POP probability can now be defined as:

$$\mathbb{P}\left(POP \,|\, \{i, j\}\right) = \mathbb{I}(c_j < t_i < c_j + a_i) \times \mathbb{P}(\{c_j, \alpha_{i,j}, s_i, r_j\} \,|\, \{t_i, a_i, s_i, r_i\}) \frac{\varphi_{\alpha_{i,j}, s_i}}{TRO_{c_j, s_i, r_j}}$$

Half-Sibling Pairs (HSPs)

The only adjustment we need to make to the HSP probability for the spatial scenario pertains to the survival of adults between the birth times of the two juvenile cohorts (i.e., point 2 of the HSP processes described above). We now need to also account for the fact that the adult could also have moved between areas during this time (and thus experienced different levels of mortality). It is a similar problem to that of the POP calculation, except we want to know the probability of where the adult will be (and if it would still be alive) conditional on the fact that, if it was a shared parent of the juveniles, it was in region r_i at time c_i and in region $r_{i'}$ at time $c_{i'}$.

As with the spatial POP probability, we set the vector $\mathbf{u}_0$ (of length 4, the number of spatial regions) as a unit vector with value 1 at location r_i and zero elsewhere. For the time periods between c_i and $c_{i'}$ we update this vector as follows:

$$u_{t+1, r} = \sum_{r'} u_{t, r'} \Phi_{r', r, a_t} \exp(-M_{a_t, s_i}) \left(1 - h_{a_t, r'}\right)$$

where $a_t = a + t$ and until $t + 1 = \delta_i - 1$ (where $\delta_i = c_{i'} - c_i$), and a is the unobserved age of the putative shared parent at time c_i. The vector $\mathbf{u}_t$ at $t = \delta_i - 1$ is the probability that the adult is both alive *and* in a specific region at that time, given it was in region r_i at time c_i. Frow this we can construct the spatially explicit HSP calculation:

$$\mathbb{P}\left(HSP \,|\, \{i, i'\}\right) = \sum_s \sum_a \left(\frac{N_{c_i, a, s, r_i} \varphi_{a, s}}{TRO_{c_i, s, r_i}} \times u_{\delta_i - 1, r_{i'}} \times \frac{\varphi_{a + \delta_i, s}}{TRO_{c_{i'}, s, r_{i'}}}\right).$$

Generating uncertainty estimates of population variables

Analyses of this kind would traditionally first simulate the data, then back-estimate the key parameters for the given models used to simulate them. If workable, this can yield both the potential

bias and parameter uncertainty properties for the pre-agreed data collection regime. This can be both difficult to do in practice (getting models to both converge and obtain uncertainty estimates for all simulated data sets), and not always necessary if previous work has explored the bias properties associated with these types of models. In this case, the predominant issue is obtaining uncertainty estimates, if either the bias properties are known (and can be accommodated), or the models are essentially unbiased for the kinds of sampling regimes under consideration.

An idea originally proposed for exploring the uncertainty of adult abundance and mortality information via close-kin mark-recapture (CKMR) was outlined in Bravington *et al.* (2016), and in a conventional spatial capture-recapture design context in Hillary & Day (2017). These models generally have a Bernoulli/binomial likelihood function as they relate to pairwise comparisons of animals and whether they are related in a specific way or not—e.g., parent-offspring. The general idea is to construct the Hessian matrix for the key estimable parameters (which defines the approximate parameter covariance matrix) via an approximation to the Fisher information (FI) at the base information level for each data source.

The Fisher information is defined in two ways. The first is in terms of the expected value of the square of the score (gradient of log-likelihood) at the maximum likelihood estimate:

$$\mathcal{I}(\boldsymbol{\theta}) = \int \left(\frac{\partial}{\partial \boldsymbol{\theta}} \ln \ell(X \mid \boldsymbol{\theta}) \right)^2 \ell(X \mid \boldsymbol{\theta}) \mathrm{d}X = \mathbb{E}^X \left[\left(\frac{\partial}{\partial \boldsymbol{\theta}} \ln \ell(X \mid \boldsymbol{\theta}) \right)^2 \right], \qquad (0.1)$$

where $\ell(X \mid \widehat{\boldsymbol{\theta}})$ is the likelihood function. The Fisher information (see further below) can also be written in terms of the second derivative of the log-likelihood (the Hessian):

$$\mathcal{I}(\boldsymbol{\theta}) = -\mathbb{E}^X \left[\frac{\partial^2}{\partial \boldsymbol{\theta}^2} \ln \ell(X \mid \boldsymbol{\theta}) \right] \qquad (0.2)$$

For a Bernoulli process with probability p, the FI is given by $1/(p(1-p))$; for a binomial process with sample size n this becomes $n/(p(1-p))$. For the Bernoulli process a conservative approximation to the FI is simply $1/p$—for things such as tag recapture data when the probability of recapture is small, this basically is a minor under-estimation (and associated minor over-estimate of uncertainty) in the FI.

In our case, the probability of occurrence is actually a function of the parameters we are really interested in, $p(\boldsymbol{\theta})$. The Fisher information of the parameter vector is defined as follows:

$$\mathcal{I}(\boldsymbol{\theta}) = \mathcal{I}(p) \left(\frac{dp}{d\boldsymbol{\theta}} \right)^2 = \frac{1}{p} \left(\frac{dp}{d\boldsymbol{\theta}} \right)^2, \qquad (0.3)$$

which, to improve numerical stability given small probabilities, can be shown (see further below) to be equivalent to the following:

$$\mathcal{I}(\boldsymbol{\theta}) = 4 \left(\frac{d\sqrt{p}}{d\boldsymbol{\theta}} \right)^{\dagger} \left(\frac{d\sqrt{p}}{d\boldsymbol{\theta}} \right) \tag{0.4}$$

This gives us the (approximate) Hessian matrix for the data at their base level covariates, $\mathbf{z}$. A very useful result is that the overall Hessian matrix, H, can be defined in terms of the sum over all the unique covariate groups of the individual Hessian matrices $H(\mathbf{z})$ as defined in (0.4):

$$H = \sum_{\mathbf{z} \in \mathcal{Z}} n^{\mathbf{z}} H(\mathbf{z}), \tag{0.5}$$

where $\mathcal{Z}$ is the set of possible covariates, and $n^{\mathbf{z}}$ is the number of observations of that covariate type in the data set. The assumed independence between the different data sets (e.g., total recaptures, spatial recapture distribution, and length frequency) means the overall Hessian matrix, from which we can form the approximate covariance of the parameter vector as a whole, is the sum of the data set specific Hessian matrices as defined in (0.5). The parameter covariance matrix, $\Sigma_{\boldsymbol{\theta}}$, is then the inverse of this overall Hessian matrix. Approximate estimates of the variance of parameters *derived* from $\boldsymbol{\theta}$ (such as spawning stock biomass, mean recruitment level, biomass depletion, and so on) via some differentiable function $g(\boldsymbol{\theta})$ can be derived with the delta method:

$$\mathbb{V}(g(\boldsymbol{\theta})) \approx \left(\frac{dg}{d\boldsymbol{\theta}} \right)^{\dagger} \Sigma_{\boldsymbol{\theta}} \left(\frac{dg}{d\boldsymbol{\theta}} \right). \tag{0.6}$$

Evidence of over-dispersion in any of the key processes (e.g. such as often encountered in conventional mark-recapture data Hillary & Day (2017)) is simple to account for in the construction of the overall Hessian matrix for the parameters. Given an estimate of the variance inflation factor, ϕ, we simply divide the Hessian matrices by the variance inflation factor, which will inflate the overall variance appropriately.

We use automatic differentiation (AD) to ensure all these calculations are done accurately, specifically the `TMB` package (Kristensen *et al.* (2016)) in R. With AD, all gradients and derived quantities are calculated to machine precision. This is a complex derivation given it leans quite heavily on statistical theory, but, once done, obtaining the uncertainty estimates of interest, given the data collection settings, becomes quick and simple relative to both simulating data and back-estimating parameter.

References

Bravington, M. V., Skaug, H. J., and Anderson, E. A. 2016. Close-kin mark recapture. *Stat. Sci.* **31**(2): 269–274.

Fu, D. *et al.*(2021) Preliminary Indian Ocean Yellowfin tuna stock assessment 1950–2020 (Stock Synthesis). *IOTC–2021–WPTT23–12*.

Hillary, R.M. and Day, J. (2017) Impact of spatial tagging rates for key estimates coming from the Macquarie Island toothfish assessment. *SARAG, AFMA, Canberra*.

Kasper Kristensen, Anders Nielsen, Casper W. Berg, Hans Skaug, Bradley M. Bell (2016). TMB: Automatic Differentiation and Laplace Approximation. Journal of Statistical Software, 70(5), 1-21. doi:10.18637/jss.v070.i05

As Australia's national science agency and innovation catalyst, CSIRO is solving the greatest challenges through innovative science and technology.

CSIRO. Unlocking a better future for everyone.

Contact us

1300 363 400
+61 3 9545 2176
csiroenquiries@csiro.au
www.csiro.au

For further information

Oceans and Atmosphere
Rich Hillary
rich.hillary@csiro.au